ChemPubSoc Europe

DOI: 10.1002/open.201600016

Open Access ChemistryOPEN Full Papers

New Synthesis of Gold- and Silver-Based Nano-Tetracycline Composites

Jamila Djafari,[a, b] Catarina Marinho,[c, d, e] Tiago Santos,[c, d, e] Gilberto Igrejas,[c, e] Carmen Torres,[f] José Luis Capelo,[a, b] Patricia Poeta,[d, e] Carlos Lodeiro,*[a, b] and Javier Fernández-Lodeiro*[a, b]

A new synthetic methodology of water-soluble gold and silver nanoparticles (AuNPs@TC and AgNPs@TC), using the antibiotic tetracycline (TC) as co-reducing and stabilizing agent, is reported. Both colloids exhibit high water stability. The average sizes obtained were 25 ± 10 and 15 ± 5 nm, respectively. Both composites were tested against TC-resistant bacteria, presenting an increasing antibacterial effect in the case of AgNPs@TC. The sensing towards metal ions was also explored. An interesting and reversible affinity of AuNPs@TC towards Al^{III} cations in an aqueous system was also observed.

1. Introduction

Silver (Ag) and gold (Au) nanoparticles (NPs) have emerged in recent decades as useful chemical tools, owing to their broad applications in medicine,[1] in (micro)biology,[2] as chemical sensors[3] and catalysts,[4] among others. The properties of Au or Ag colloidal systems are a combination of the Au and Ag own properties and the properties created by the molecular system used to decorate them when the nanomaterial is made.

[a] J. Djafari, Dr. J. L. Capelo, Dr. C. Lodeiro, Dr. J. Fernández-Lodeiro
BIOSCOPE Group, UCIBIO@REQUIMTE
Chemistry Department, Faculty of Science and Technology
University NOVA of Lisbon, 2829-516 Monte da Caparica (Portugal)
E-mail: clodeiro@bioscopegroup.org
j.lodeiro@fct.unl.pt

[b] J. Djafari, Dr. J. L. Capelo, Dr. C. Lodeiro, Dr. J. Fernández-Lodeiro
ProteoMass Scientific Society, Faculty of Sciences and Technology
University NOVA of Lisbon, Madan Parque. Building VI. Office 23
2829-516 Monte da Caparica (Portugal)

[c] C. Marinho, T. Santos, Dr. G. Igrejas
Functional Genomics and Proteomics Unit
Department of Genetics and Biotechnology
University of Trás-os-Montes and Alto Douro, 5000-801 Vila Real (Portugal)

[d] C. Marinho, T. Santos, Dr. P. Poeta
Veterinary Science Department
University of Trás-os-Montes and Alto Douro, 5000-801 Vila Real (Portugal)

[e] C. Marinho, T. Santos, Dr. G. Igrejas, Dr. P. Poeta
UCIBIO@REQUIMTE, Chemistry Department
Faculty of Science and Technology, University NOVA of Lisbon
2829-516 Monte da Caparica (Portugal)

[f] Dr. C. Torres
Department of Food and Agriculture, Biochemistry and Molecular Biology
University of La Rioja (UR), 26006 Logroño (Spain)

Supporting Information and the ORCID identification number(s) for the author(s) of this article can be found under http://dx.doi.org/10.1002/open.201600016.

Ag and Au metal NPs present extraordinary size-dependent optoelectronic properties, derived from the collective oscillation of conduction electrons produced by visible light. This phenomenon is known as surface plasmon resonance (SPR). The SPR is tunable, and thus the frequency can be modified by changes in NP composition, size, shape, or spatial disposition.[5]

In addition, metal NPs are sensitive to their local environment. The aforementioned phenomena have opened new possibilities for using such NPs as new chemo-nano-sensors.[6] Further important intrinsic characteristics of this type of nanomaterial are its oxidative properties, its chemical affinity, and its chemical reactivity. Moreover, the nanoscale dimension allows implementation in biological and biomedical applications.[7] In addition, the properties of these nanomaterials can be modulated through specific functionalization.[8]

Reports about the functionalization of pre-synthesized AgNPs with tetracycline (TC) have been described recently,[9,10] and Shen and co-workers have reported the ability of TC to reduce Au under specific conditions.[11] To the best to our knowledge, the simultaneous synthesis of AgNPS by using TC as a co-reducer and stabilizing agent has not previously been reported. Thus, following our research line in functionalized nanomaterials,[12] we report the first synthesis of gold- and silver-based nano-TC composites.

2. Results and Discussion

2.1. Synthesis of AgNPs@TC and AuNPs@TC

Nishimura et al. have reported that the pH of the medium can control the reduction of Ag ions in the presence of complexing molecules.[13] By using this strategy, we synthetized Ag NPs with TC in basic pH conditions under temperature stimulation. These nanocomposites can be stabilized and functionalized with TC through weak bonds in a simple procedure. TC is a complex molecule with different tautomeric forms, which

makes it difficult to determine the structure on the surface of the NPs. However, we assume that TC can interact with Ag ions at the amide position, owing to the affinity observed between Ag ions and the amide group.[14] TC presents four acidic hydrogens, which can deprotonate in water, Ha, Hb, Hc, and Hd, with pK_a values of 3.3, 7.3, 9.0, and 11.8 respectively (see Figure S1 in the Supporting Information).[15]

The protonated species of TC shows very low solubility in water. By using sodium hydroxide as a strong base, it is possible to deprotonate the molecule, reducing the Ag ions present in solution at the same time.

Figure S2 depicts a NaOH-based UV/Vis titration of TC in DMSO (1.10^{-5} M). The presence of four isosbestic points at approximately 265, 282, 305, and 376 nm confirms the presence of different deprotonated species in water. The system is fully stabilized with the addition of three equivalents of NaOH. To ensure the effective deprotonation of the TC, four equivalents of NaOH were used in our experiments. We observed that the optimal molar ratio of $AgNO_3$/TC/NaOH for the synthesis of these NPs was 1:6:24.

The reaction was carried out at boiling temperature to promote silver nitrate reduction. Preheated (80 °C) basic TC solution was rapidly added to the boiled silver solution. A rapid addition of the preheated solution should create a lower temperature gradient, shortening the nucleation process. This reaction solution exhibits a yellow/brown color. After two centrifugation cycles, the AgNPs@TC colloidal system presents the characteristic yellow color of Ag colloids. The AgNPs@TC composites presents an intense SPR band centered at about 403 nm. By using transmission electron microscopy (TEM), a quasi-spherical shape with an average size of 15 ± 5 nm was observed (see Figure 1 a).

The yellow colloidal water solution was stable for several weeks. The properties of this colloidal solution are pH dependent. Indeed, according to our UV/Vis studies, an intense SPR band is observed at about 403 nm at pH 5.5. For a pH value lower than 4, a decrease in intensity of the SPR band centered about 403 nm is observed, and a new SPR band centered at about 474 nm appears simultaneously. This colloidal solution changes from yellow to orange (see Figure 2 a). This phenomenon is attributed to a plasmonic coupling of discrete units of NPs. This coupling takes place as a result of the protonation of the pH-dependent sites present on TC, leading to a decrease in the formal charge of the NP surface. This observation is consistent with the protonation values of TC obtained in the literature.

A study of the zeta potential (Z) versus pH was performed to confirm the above hypothesis. Between pH 4 and 12, the AgNPs@TC composites show a negative surface charge ranging between −32 and −28 mV. This further confirms the stabilization of the colloidal system by the negative charges located on the TC. However, at acidic values, between pH 2 and 4, the zeta potential was close to zero, and thus there are no charges stabilizing the particles. This increases particle aggregation. This aggregation is observed with the naked eye by the color change from yellow to orange, as mentioned above. These findings are in agreement with the pK_a values of the TC; in fact, at pH values lower than 3.3, TC should be fully protonated (see Figure 2 a). To compare the antibacterial activity of AgNPs@TC composites, AuNPs@TC NPs were synthesized following the same protocol. This Au-based nanocomposite was synthetized to control whether the antibacterial activity of the Ag-based nanocomposite was influenced by free Ag ions.[16] It is well known that gold is biocompatible, thus exhibiting low antibacterial activity.[17] The functionalized AuNPs@TC material

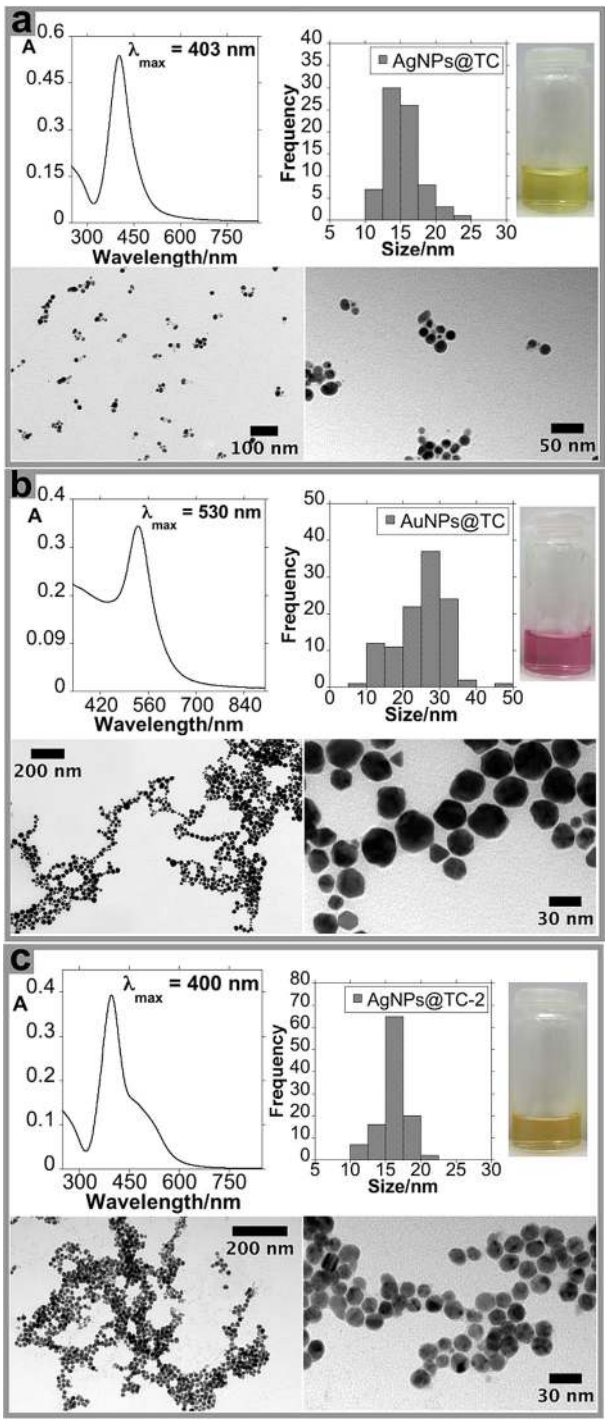

Figure 1. UV/Vis absorption spectra, color solution, histogram, and TEM images of AgNPs@TC (a), AuNPs@TC (b), and AgNPs@TC-2 (c).

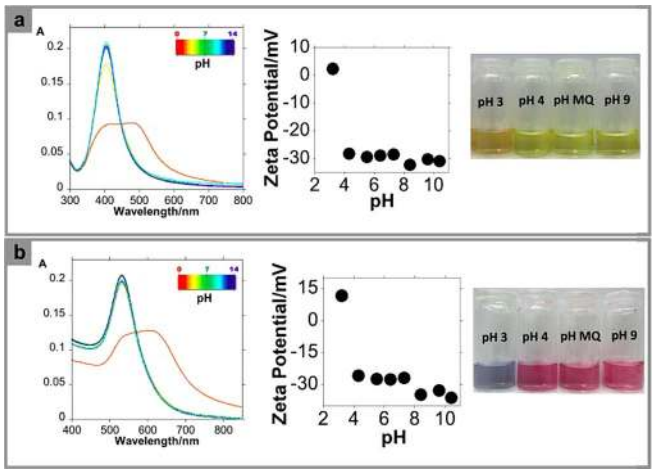

Figure 2. UV/Vis absorption spectra, *Z* potential and color solution of AgNPs@TC (a) and AuNPs@TC (b) as a function of pH (pH between 2 and 11).

presents an SPR band at about 530 nm, as confirmed by their pink–red color. This result is in agreement with the average size of these gold NPs, 25 ± 10 nm (see Figure 1 b). As it was observed previously with the AgNPs@TC, the AuNPs@TC properties are pH dependent in water (see Figure 2 b). TC shows different stability depending on the reaction time and temperature used. As previously reported in the literature, TC has a stronger sensitivity to moderate temperature for longer periods than to higher temperature for short periods of time. Eisenhart et al. have previously reported that 90% of the TC ligand is stable for 1 h at 90 °C.[18] TC is also sensitive to light radiation.[19] Taking this information in mind, a second batch of AgNPs@TC-2 was prepared. Now the reaction time was 15 min, and the synthesis was carried out in the dark. We observed a decrease in the yield of nanomaterial obtained under such conditions. The spectroscopic profile shows a SPR band centered at 400 nm with a shoulder at higher wavenumber. TEM images showed a greater degree of monodispersity when compared to AgNPs@TC (see Figure 1 c).

2.2. Metal Sensing Applications

It is well documented that free TC shows effective interactions with divalent and trivalent metal cations in solution.[20,21] To determine any potential metallic interferences during the bacterial studies, and to explore the application as a nanosensor in water, both metallic composites were studied in the presence of Na^+, K^+, Hg^+, Mg^{2+}, Ca^{2+}, Mn^{2+}, Cu^{2+}, Zn^{2+}, Cd^{2+}, Hg^{2+}, Pb^{2+}, Cr^{3+}, Fe^{2+}, Fe^{3+}, Al^{3+}, Ga^{3+}, and In^{3+} ions. Under our conditions, neither of the systems shows any remarkable interaction with the metal ions studied, with the exception of trivalent cations. The strongest affinity was observed towards Al^{3+}. It is interesting to note that the pink–red colloidal solution of AuNPs@TC shows greater sensitivity (nM range) towards this metal when compared to the AgNPs@TC system (μM range). Moreover, the addition of 500 nM Ga^{3+} or 500 nM In^{3+} promotes a change in the color from red to violet (see Figure S3). The results obtained for the AgNPs@TC composites are showed in Figure S4.

As a result of the interaction between Al^{3+} and the AuNPs@TC system, the SPR bands shifted to lower energy values (redshift). This confirms the aggregation as a result of lower negative surface charge.

The net negative charged surface in the gold system, owing to the presence of the TC oxygen atoms, produces a high affinity for trivalent metal cations. Moreover, the larger size obtained with the AuNPs@TC composite induces an increase in sensitivity when compared with the smaller silver material. The increase in the average size of NPs produces a lower surface area of the resulting colloidal system, indicating minor TC molecules functionalized onto the surface of the NPs.

With the intention of generating a naked-eye colorimetric system, solutions with different SPR absorptions were used. The AuNPs@TC solution producing a color that can be seeing by the naked eye has an absorption value of 0.2 (see Figure 3 a). Spectroscopic studies using solutions with lower SPR absorption (0.1) showed an improvement in sensitivity towards Al^{3+}. However, solutions with low SPR absorption cannot be seen by the naked eye (see Figure S5).

The naked-eye sensing ability for Al^{3+} was observed for aluminum concentrations ranging between 200 and 500 nM. Below 200 nM, the AuNPs@TC exhibits a pink color, moving to blue for Al^{3+} concentrations between 200 and 500 nM. For concentrations higher than 500 nM, the system moves to blue (see Figure 3 a and Figure S6).

As can be seen in Figure 3 b, large NP aggregates were observed when the AuNPs@TC composite was mixed with a 500 nM Al^{3+} solution. The spatial arrangement of the colloidal system in solution was studied by dynamic light scattering (DLS) analysis. A value of 34.03 nm (volume distribution data) was obtained for the free AuNPs@TC composite. Following the addition of 500 nM of Al^{3+}, this value increases to 381.73 nm (volume distribution data). The formation of aggregates in solution produced by the interaction with Al^{3+} is supported by the results obtained in the analysis of *Z* potential. Indeed, the *Z* potential of the AuNPs@TC system presents a value of $-27.4\ mV\,cm^{-1}$, and this value rises to $-14.16\ mV\,cm^{-1}$ after the addition of 500 nM Al^{3+}.

To explore the reversibility, the AuNPs@TC-Al colloidal system was treated with an EDTA solution. Interestingly, our system recovers its initial optical properties as a result of the complexation of Al^{3+} cations by the EDTA molecule (see Figure 3 b and Scheme 1).

2.3. Exploring Antibacterial Activity

As a potential application, the NPs were tested as a bactericidal. To this end, *E. coli* and *S. aureus* bacteria, susceptible to TC or resistant to TC, were used. The AuNPs@TC composites were not found to be bactericidal (data shown in Table 1, MBC) and were also not able to inhibit the growth of *E. coli* and *S. aureus* resistant to TC. However, these NPs were able to inhibit the growth of susceptible *E. coli* and *S. aureus*. AgNPs@TC composites were found to inhibit growth as well as to kill 1) *E. coli*

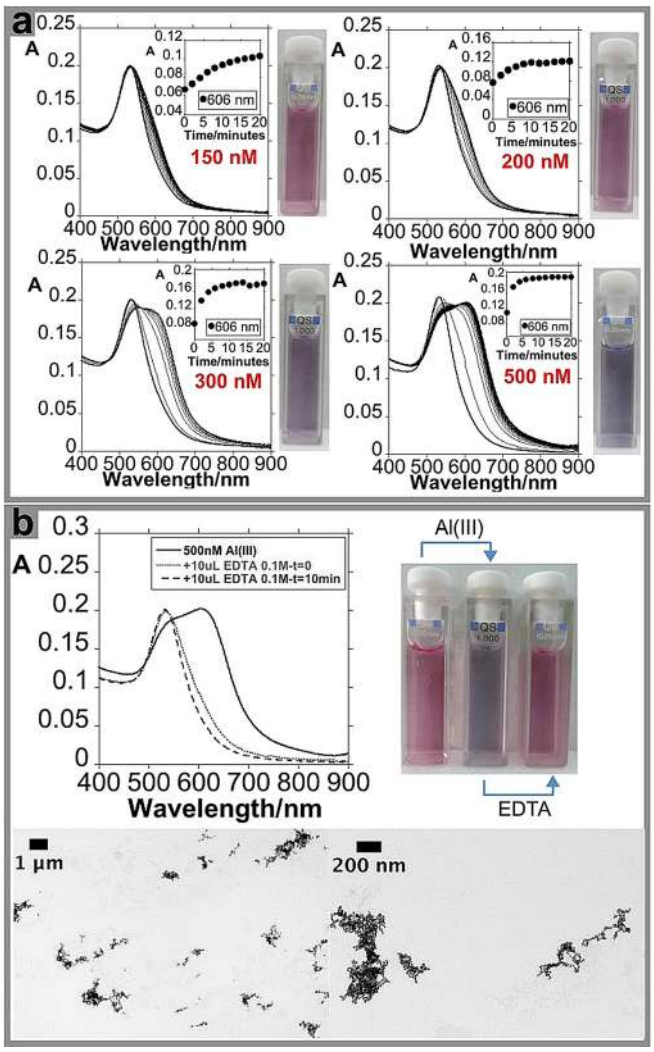

Figure 3. Spectrophotometric titration of AuNPs@TC with the addition of increasing amounts of $Al(NO_3)_3$ and naked-eye detection (a). Reversible colorimetric change upon addition of EDTA in aqueous solution and TEM images of AuNPs@TC with the addition of 500 nM of $Al(NO_3)_3$ (b).

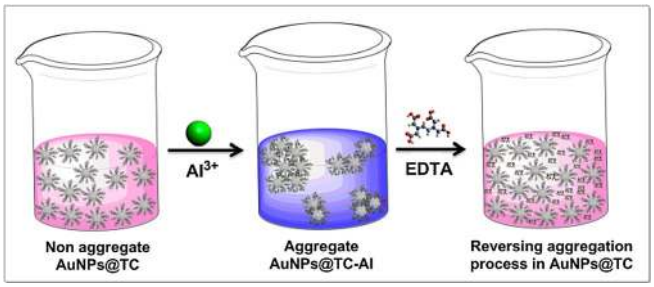

Scheme 1. Illustrative representation of reversible naked-eye sensing of AuNPs@TC towards Al^{3+}.

susceptible and resistant to TC, and 2) *S. aureus* susceptible to TC. The best performance was obtained with the AgNP@TC-2 composite, as it was found to inhibit and to kill *E. coli* susceptible and resistant to TC as well as *S. aureus* susceptible to TC. However, it fails to kill TC-resistant *S. aureus* at the maximum assayed concentration level. When the bactericidal effects of the nanocomposites are compared with that of TC alone, the amount of TC required is equal or considerably lower. This finding is in agreement with previous studies.[24,25]

Table 1. Antimicrobial effect of NPs functionalized with TC, on TC-susceptible and -resistant *E. coli* and *S. aureus* strains. (S-susceptible to TC; R-resistant to TC; ND-not determined).

NP sample	Strain	MIC [μg mL^{-1}]	MBC [μg mL^{-1}]	pH
AuNPs@TC	*E. coli* K12 ATCC 29425 (S)	6	ND	6.8
	E. coli ST648 (R)	ND	ND	6.8
	S. aureus ATCC 25923 (S)	16	ND	6.6
	S. aureus ST398 (R)	ND	ND	6.6
AgNPs@TC	*E. coli* K12 ATCC 29425 (S)	16	20	6.8
	E. coli ST648 (R)	25	35.5	6.8
	S. aureus ATCC 25923 (S)	16	35.5	6.8
	S. aureus ST398 (R)	ND	ND	7.0
AgNPs@TC-2	*E. coli* K12 ATCC 29425 (S)	32	32	7.2
	E. coli ST648 (R)	40	40	6.8
	S. aureus ATCC 25923 (S)	32	40	7.0
	S. aureus ST398 (R)	62.3	ND	6.8
TC	*E. coli* K12 ATCC 29425 (S)	0.5	16	6.4
	E. coli ST648 (R)	128	256	6.0
	S. aureus ATCC 25923 (S)	8	128	6.8
	S. aureus ST398 (R)	64	256	6.0
AgNPs 15 nm[22]	*E. coli* ATCC 25922[23] (S)	30	50	ND
	E. coli ATCC 10536 (S)	90	110	ND
	S. aureus ATCC 25923 (S)	100	110	ND

Gold NPs are known to be non-cytotoxic, biocompatible, and useful therapeutic drug-delivery vehicles.[17,26,27] In this context, we determined that AuNPs@TC is, in fact, nontoxic to bacteria, as it was possible to recover viable bacteria after 36 h of growth in the presence of our AuNPs@TC composite. Although it is not bactericidal, gold NPs functionalized with TC are capable of inhibiting TC-susceptible Gram-negative and Gram-positive bacteria.

Silver NPs are effective antimicrobial agents, despite the adverse effects of toxicity to both bacteria and eukaryotic cells. In contrast, the cytotoxicity of gold NPs is quite low.[24,26] Our results are in agreement with these facts, as AgNPs@TC showed an improved bactericidal capability than the gold NPs, which may arise from the cytotoxicity of silver instead of the nontoxicity of gold. We concluded that the highest concentration of Ag NPs in AgNPs@TC solutions leads to a greater bactericidal and inhibitory effect. As was previously reported, the synergistic effect of Ag and TC is evident in our results, as AgNPs@TC solutions had a largely enhanced bactericidal proficiency compared to TC.[28] The synergistic effect of Ag and TC is also demonstrated by comparing microbiological results with those present in the literature by using antibacterial Ag NPs of a similar size, without TC and stabilized by citrate molecules, against the same bacteria (different strains).[22] By analyzing the minimum inhibitory concentration (MIC) and minimum bactericidal concentration (MBC) values obtained, our AgNPs@TC compo-

site exhibits better antibacterial activity against Gram-negative and Gram-positive bacteria compared to the Ag NPs stabilized by an innocent citrate molecule, which requires a higher concentration to inhibit bacteria growth.

3. Conclusions

A new one-pot method for the synthesis of Au and Ag NPs, using TC and sodium hydroxide, has been described. The new method is less time consuming, requires less handling, and ensures that all of the TC used is attached to the composite. The nanocomposites are stable for several weeks. The average composite sizes (25 ± 10 and 15 ± 5 nm, for Au and Ag NPs, respectively) guarantees an area-to-volume ratio appropriate to deliver TC in a quantity sufficient to kill bacteria. Remarkably, the AgNPs@TC-2 system shows bactericidal abilities against Gram-negative and Gram-positive TC-susceptible and TC-resistant bacteria, with better results than TC-free and Ag NP equivalents. An additional feature of the nanocomposites described here is the enormous sensitivity and selectivity towards Al^{3+} in water. This finding opens the possibility to use this gold system as a reversible colorimetric Al^{3+} nanosensor. Further studies are in progress, focusing on the functionalization of Ag and Au NPs with other specific antibiotics.

Experimental Section

Chemicals Materials

Silver nitrate ($AgNO_3$), tetrachloroauric (III) acid ($HAuCl_4.3\,H_2O$), TC, sodium hydroxide (NaOH), hydrochloric acid (HCl), sodium chloride (NaCl), potassium chloride (KCl), mercury(I) chloride (HgCl), magnesium(II) trifluoromethanesulfonate [$Mg(OTf)_2$], calcium trifluoromethanesulfonate [$Ca(OTf)_2$], manganese(II) nitrate tetrahydrate [$Mn(NO_3)_2.4\,H_2O$], copper(II) nitrate hexahydrate [$Cu(NO_3)_2.6\,H_2O$], zinc chloride ($ZnCl_2$), cadmium(II) trifluoromethanesulfonate [$Cd(OTf)_2$], mercury(II) chloride ($HgCl_2$), lead(II) trifluoromethanesulfonate [$Pb(OTf)_2$], chromium(III) nitrate hexahydrate [$Cr(NO_3)_2.6\,H_2O$], iron(III) chloride hexahydrate ($FeCl_3.6\,H_2O$), aluminum nitrate hexahydrate [$Al(NO_3)_2.6\,H_2O$], gallium(III) nitrate hexahydrate [$Ga(NO_3)_2.6\,H_2O$], indium(III) perchlorate octahydrate [$In(ClO_4)_3.8\,H_2O$], and ethylenediaminetetraacetic acid (EDTA) were purchased from Sigma Aldrich, Strem Chemicals, Fluka, or Panreac, and used without further purifications.

Water was always Milli-Q grade by Millipore.

The pH value of aqueous solutions was adjusted by using concentrated solutions of NaOH and HCl. The pH was measured through potentiometry.

Preparation of AgNPs@TC

In a two-necked round-bottom flask, a solution of silver nitrate (4.10^{-4} M) in 50 mL Milli-Q water was heated to the boiling point. Then, a pre-heated (80 °C) mixture of 20 mL of TC (6.10^{-3} M, 6 equiv) and NaOH ($2.4.10^{-2}$ M, 24 equiv) was added into the solution. The firstly yellow solution turned dark red after the addition of the alkaline solution, owing to the silver nitrate reduction. Then, it turned dark brown. The solution was refluxed for 2 h. The round-bottom flask was then cooled in an ice/water bath. The NPs were separated from the supernatant by centrifugation twice at 8000 rpm for 1 h. The pellet was washed once with Milli-Q water at 8000 rpm for 30 min. The final yellow NPs were re-suspended in 15 mL Milli-Q water.

Preparation of AgNPs@TC-2

In a two-necked round bottom flask, a light-protected solution of silver nitrate (4.10^{-4} M) in 50 mL Milli-Q water was heated to the boiling point. Then, a boiled mixture of 20 mL of TC (6.10^{-3} M, 6 equiv) and NaOH ($2.4.10^{-2}$ M, 24 equiv) was added into the solution. The firstly yellow solution became dark red after the addition of the alkaline solution, owing to the silver nitrate reduction. Then, it became red–brown. The solution was refluxed for 15 min in darkness. The round-bottom flask was then cooled in an ice/water bath. The NPs were separated from the supernatant by centrifugation, twice at 8000 rpm for 1 h. The pellet was washed once with Milli-Q water at 8000 rpm for 30 min. The final orange NPs were re-suspended in 15 mL Milli-Q water.

Preparation of AuNPs@TC

In a two-necked round bottom flask, a solution of tetrachloroauric(III) acid (4.10^{-4} M) in 50 mL Milli-Q water was heated to the boiling point. Then, a boiled mixture of 20 mL of TC (6.10^{-3} M, 6 equiv) and NaOH ($2.4.10^{-2}$ M, 24 equiv) was added into the solution. The firstly yellow solution became dark red after the addition of the alkaline solution, owing to gold complex formation. Then, it became dark brown. The solution was refluxed for 2 h. The round-bottom flask was then cooled in an ice/water bath. The NPs were separated from the supernatant by centrifugation, twice at 10000 rpm for 1 h. The pellet was washed once with Milli-Q water at 10000 rpm for 30 min. The final red–pink NPs were re-suspended in 15 mL Milli-Q water.

Spectrophotometric Measurements

Electronic absorption spectra of the NPs were recorded by using Jasco V-630 and Jasco V-650 UV/Vis spectrophotometers (Easton, MD, UK from the Proteomass-BIOSCOPE Facility lab). In both cases, the spectrophotometric characterization and titrations were performed by preparing stock solutions in milli-Q water in 10 mL volumetric flasks. The studied solutions were prepared by appropriate dilution of the stock solutions. In all cases, 1 cm optical-path quartz cells were used (Hellma QXX).

To determine the coordinative characteristics of the functionalized NPs and sensorial effects, the absorption spectra in the absence and in the presence of a known concentration of different metal ions (Na^+, K^+, Hg^+, Mg^{2+}, Ca^{2+}, Mn^{2+}, Cu^{2+}, Zn^{2+}, Cd^{2+}, Hg^{2+}, Pb^{2+}, Cr^{3+}, Fe^{3+}, Al^{3+}, Ga^{3+}, and In^{3+}) were recorded. The spectra were recorded with the increased addition of metal ions. All measurements were performed at a controlled temperature of 298 K.

DLS and *Z* Potential Measurement

The *Z* potential of each sample was measured by using a Malvern Zetasizer Nano series (Worcestershire, WR14 1XZ, UK) from Proteomass Scientific Society–BIOSCOPE Facility Lab. The measured solution was obtained by centrifugation for 10 min at 8000 rpm, and the obtained pellet was re-suspended in the previously prepared pH solution. Samples were analyzed by using a folded capillary cell at room temperature.

TEM Measurements

The TEM images were obtained by using a JEOL JEM 1010F transmission electron microscope from the CACTI, University of Vigo (Spain), operating at 100 kV. Samples were prepared by dropping 5 μL of the colloidal suspension on a copper grid coated with a continuous carbon film, and the solvent was allowed to evaporate. TEM images were characterized by using Image J software. Histograms were prepared by counting a minimum of 100 NPs per sample.

Metals Screening—CLARIOstar

The screening of metals ions was performed by using a CLARIOstar system, BMG Labtech (220–900 nm) in water from the Proteomass Scientific Society–BIOSCOPE Facility Lab. The studies were carried out by preparing aqueous solutions of metals with concentrations between 1.10^{-3} and 1.10^{-4} M. Concentrations of NPs were normalized to have an absorbance equal to 0.2. By using the 96-well-plate CLARIOstar system, the NPs were added to wells with the required amount of each metal.

NPs Concentration and Inductively Coupled Plasma–Atomic Emission Determination

The Ag concentration in the AgNPs@TC samples was determined by using inductively coupled plasma analysis, using an Horiba Jobin–Yvon (France, model Ultima), equipped with an RF of 40.68 MHz, a 1.00 m Czerny–Turner monochromator (sequential), and an AS500 autosampler. Concomitant metals analysis for the determination of the simultaneous presence of Hg, As, Se, Sb, and Sn was perform in the REQUIMTE-FCT-UNL analytical laboratory.

The total NP concentration (NPs + TC) was calculated by drying 1 mL of a lyophilized solution of NPs in an Eppendorf tube. The obtained solid was weighed with a Mettler Toledo, Model AT21, microbalance.

Bacteria and Growth Conditions

Bacterial strains considered in this study are described in Table 2. Strains tested were *E. coli* ST648 and *S. aureus* ST398, both resistant to TC, and the control strains *E. coli* K12 and *S. aureus* ATCC 25923, susceptible to TC. Bacteria were seeded on BHI medium agar (Oxoid) and incubated at 35 °C ± 2 °C for 18–20 h.

Table 2. Bacterial strains used in this study.

Strain	Relevant phenotype[a]	Reference
E. coli K12 ATCC 29425	Non-pathogenic, Gram negative; Tet^s	ATCC
E. coli ST648	Pathogenic, Gram negative; Tet^r	[30]
S. aureus ATCC 25923	Gram positive; Tet^s	ATCC
S. aureus ST398	Pathogenic, Gram positive; Tet^r	[31]

[a] Tet^s, TC sensitive; Tet^r, resistant to TC.

Preparation of Antibiotic and NP Stock Solutions

The AuNPs@TC solution was diluted to 60.9, 45.7, and a 32–0.125 μg mL^{-1} range, and tested on all bacteria. The AgNPs@TC (sample 1) solution was diluted to 35.5, 26.6, 25, 20, and a 16–0.25 μg mL^{-1} range, and tested on all bacteria. The AgNPsTC-2 (sample 2) solution was diluted to 62.3, 46.7, 40, and a 32–0.25 μg mL^{-1} range, and tested on all bacteria. TC was tested on a range of 256–0.25 μg mL^{-1} for *E. coli* and 1024–0.5 μg mL^{-1} for *S. aureus*. Positive (inoculated medium) and negative controls (medium supplemented with NPs/antibiotic) were included for all tests. All tests were performed in triplicate.

Determination of the MIC of the NPs

The MIC assay was determined by using the broth-microdilution method to determine antimicrobial effect of thee functionalized NPs on *S. aureus* and *E. coli*.[29] A total of three 96-well sterile microliter trays were filled with 100 μL of Luria–Bertani (LB) broth medium (Sigma–Adrich) and appropriate antibiotic dilutions. Each set was inoculated aseptically with 10 μL of respective bacterial suspension (10^6 CFU mL^{-1}). An antibiotic-free control row was considered in each plate. The pH measurement was determined for the first dilution well in each row, after inoculation.

Plates were sealed with Parafilm and incubated with shaking at 35 °C ± 2 °C for 18–20 h with aeration. Each experiment was performed in duplicate. MICs were recorded by the naked eye determining the lowest concentration that locked bacteria growth.

The effect of NPs on individual bacterial isolates was determined according to the following protocol. The 18 h cultures of bacterial strains that resulted from MIC testing were directly inoculated in fresh LB medium on 60 mm × 15 mm plates (100 μL total per sample). Control cultures without NPs were included in all experiments. The number of colony-forming units (CFUs) recovered after incubation for 18–20 h at 35 °C ± 2 °C with aeration was determined by plate counting. The number of bacteria present in the inoculum was determined for each strain in each experiment. The colonies present on LB plates for each dilution per sample were counted and the presence/absence was registered.

The MBC is the lowest concentration of NPs that resulted in no bacterial growth after 18 h of incubation at 37 °C. Each experiment was performed in duplicate.

Acknowledgements

J.D., C.L,. and J.F.-L. conceived and designed the experiments; J.D. and J.F.-L. performed the synthesis and characterization of the TC functionalized Ag and Au NPs, as well as the metal-ion sensing studies. C.M., T.S., G.I., and P.P. studied the bacterial interactions with the NPs. C.T. provided the TC bacterial resistant strains. All authors have analyzed the data. J.F.L., J.D., C.L, J.L.-C., C.M., P.P., and G.I. wrote and corrected the paper. C.L., J.L.-C., G.I., and P.P. contributed with reagents/materials/analysis tools. J.F.-L. thanks Fundação para a Ciência e a Tecnologia- Ministério de Ciência e Educação (FCT/MEC) (Portugal) for his postdoctoral grant reference SFRH/BPD/93982/2013. J.D. thanks Proteomass Scientific Society for a PhD research grant. This work was supported by the Associate Laboratory for Green Chemistry LAQV, which is financed by national funds from FCT/MEC (UID/QUI/50006/2013) and co-financed by the European Regional Development Fund (ERDF) under the PT2020 Partnership Agreement (POCI-01–0145-FEDER-007265) and by the Unidade de Ciências Biomoleculares

Aplicadas–UCIBIO, which is financed by national funds from FCT/MEC (UID/Multi/04378/2013) and co-financed by the ERDF under the PT2020 Partnership Agreement (POCI-01-0145-FEDER-007728). All authors thank the Proteomass Scientific Society, General Funds (Portugal) for financial support.

Keywords: aluminum detection · antimicrobial studies · gold and silver nanoparticles · nanoantibiotics · nanochemical sensor

[1] a) V. K. Sharma, R. A. Yngard, Y. Lin, *Adv. Colloid Interface Sci.* **2009**, *145*, 83 – 96; b) L. A. Dykman, N. G. Khlebtsov, *Chem. Soc. Rev.* **2012**, *41*, 2256 – 2282.

[2] a) J. R. Morones, J. L. Elechiguerra, A. Camacho, K. Holt, J. B. Kouri, J. T. Ramirez, M. J. Yacaman, *Nanotechnology* **2005**, *16*, 2346 – 2353; b) D. A. Giljohann, D. S. Seferos, W. L. Daniel, M. D. Massich, P. C. Patel, C. A. Mirkin, *Angew. Chem. Int. Ed.* **2010**, *49*, 3280 – 3294; *Angew. Chem.* **2010**, *122*, 3352 – 3366.

[3] a) A. D. McFarland, R. P. Van Duyne, *Nano Lett.* **2003**, *3*, 1057 – 1062; b) K. Saha, S. S. Agasti, C. Kim, X. Li, V. M. Rotello, *Chem. Rev.* **2012**, *112*, 2739 – 2779.

[4] a) Z. J. Jiang, C. Y. Liu, L. W. Sun, *J. Phys. Chem. B* **2005**, *109*, 1730 – 1735; b) M. C. Daniel, D. Astruc, *Chem. Rev.* **2004**, *104*, 293 – 346.

[5] K. A. Willets, R. P. Van Duyne, *Annu. Rev. Phys. Chem.* **2007**, *58*, 267 – 297.

[6] B. Sepúlveda, P. C. Angelomé, L. M. Lechuga, L. M. Liz-Marzán, *Nano Today* **2009**, *4*, 244 – 251.

[7] P. K. Jain, X. Huang, I. H. El-Sayed, M. A. El-Sayed, *Acc. Chem. Res.* **2008**, *41*, 1578 – 1586.

[8] R. Mout, D. F. Moyano, S. Rana, V. M. Rotello, *Chem. Soc. Rev.* **2012**, *41*, 2539 – 2544.

[9] A. J. Kora, L. Rastogi, *Bioinorg. Chem. Appl.* **2013**, *2013*, 871097.

[10] C. Khurana, A. K. Vala, N. Andhariya, O. P. Pandey, B. Chudasama, *Environ. Sci.: Processes Impacts* **2014**, *16*, 2191 – 2198.

[11] L. Shen, J. Chen, N. Li, P. He, Z. Li, *Anal. Chim. Acta* **2014**, *839*, 83 – 90.

[12] a) A. Fernández-Lodeiro, J. Fernández-Lodeiro, C. Núñez, R. Bastida, J. L. Capelo, C. Lodeiro, *ChemistryOpen* **2013**, *2*, 200 – 207; b) C. I. M. Santos, E. Oliveira, J. Fernández-Lodeiro, J. F. B. Barata, S. M. Santos, M. A. F. Faustino, J. A. S. Cavaleiro, M. G. P. M. S. Neves, C. Lodeiro, *Inorg. Chem.* **2013**, *52*, 8564 – 8572; c) J. Fernández-Lodeiro, C. Núñez, E. Oliveira, J. L. Capelo, C. Lodeiro, *J. Nanopart. Res.* **2013**, *15*, 1828 – 1837; d) J. Fernández-Lodeiro, C. Núñez, A. Fernández-Lodeiro, E. Oliveira, B. Rodriguez, A. Dos Santos, J. L. Capelo, C. Lodeiro, *J. Nanopart. Res.* **2014**, *16*, 2315 – 2327; e) J. E. Araújo, C. Lodeiro, J. L. Capelo, B. Rodríguez-González, A. Dos Santos, H. M. Santos, J. Fernández-Lodeiro, *Nano Res.* **2015**, *8*, 1189 – 1198.

[13] S. Nishimura, D. Mott, A. Takagaki, S. Maenosono, K. Ebitani, *Phys. Chem. Chem. Phys.* **2011**, *13*, 9335 – 9343.

[14] V. Romanov, C. K. Siu, U. H. Verkerk, H. El Aribi, A. C. Hopkinson, K. W. M. Siu, *J. Phys. Chem. A* **2008**, *112*, 10912 – 10920.

[15] A. Amat, S. Fantacci, F. De Angelis, B. Carlotti, F. Elisei, *Theor. Chem. Acc.* **2012**, *131*, 1218 – 1231.

[16] Z. M. Xiu, Q. B. Zhang, H. L. Puppala, V. L. Colvin, J. J. P. Alvarez, *Nano Lett.* **2012**, *12*, 4271 – 4275.

[17] P. Ghosh, G. Han, M. De, C. K. Kim, V. M. Rotello, *Adv. Drug Delivery Rev.* **2008**, *60*, 1307 – 1315.

[18] a) A. E. Eisenhart, N. M. Disso, *Proceedings of the National Conference On Undergraduate Research* **2012**, 350 – 356; b) M. Hassani, R. Lázaro, C. Pérez, S. Condón, R. Pagán, *J. Agric. Food Chem.* **2008**, 2676 – 2680.

[19] H. Oka, Y. Ikai, N. Kawamura, M. Yamada, K. Harada, S. Ito, M. Suzuki, *J. Agric. Food Chem.* **1989**, *37*, 226 – 231.

[20] I. Chopra, M. Roberts, *Microbiol. Mol. Biol. Rev.* **2001**, *65*, 232 – 260.

[21] M. L. Nelson, W. Hillen, R. A. Greenwald, *Tetracyclines in Biology, Chemistry and Medicine*, Birkhäuser, Basel, **2001**.

[22] S. Agnihotri, S. Mukherji, S. Mukherji, *RSC Adv.* **2014**, *4*, 3974 – 3983.

[23] T. D. Minogue, H. A. Daligault, K. W. Davenport, K. A. Bishop-Lilly, S. M. Broomall, D. C. Bruce, P. S. Chain, O. Chertkov, S. R. Coyne, T. Freitas, K. G. Frey, H. S. Gibbons, J. Jaissle, C. L. Redden, C. N. Rosenzweig, Y. Xu, S. L. Johnson, *Genome Announc.* **2014**, *2*, e00969 – 14.

[24] A. N. Brown, K. Smith, T. A. Samuels, J. Lu, S. O. Obare, M. E. Scott, *Appl. Environ. Microbiol.* **2012**, *78*, 2768 – 2774.

[25] L. Wang, Y. P. Chen, K. P. Miller, B. M. Cash, S. Jones, S. Glenn, B. C. Benicewicz, A. W. Decho, *Chem. Commun.* **2014**, *50*, 12030 – 12033.

[26] X. Li, S. M. Robinson, A. Gupta, K. Saha, Z. Jiang, D. F. Moyano, A. Sahar, M. A. Riley, V. M. Rotello, *ACS Nano* **2014**, *8*, 10682 – 10686.

[27] L. A. Dykman, N. G. Khlebtsov, *Acta Naturae* **2011**, *3*, 34 – 55.

[28] A. M. Fayaz, K. Balaji, M. Girilal, R. Yadav, P. T. Kalaichelvan, R. Venketesan, *Nanomedicine* **2010**, *6*, 103 – 109.

[29] J. M. Andrews, *J. Antimicrob. Chemother.* **2001**, *48*, 5 – 16.

[30] E. Ruiz, Y. Saenz, M. Zarazaga, R. Rocha-Gracia, L. Martinez-Martinez, G. Arlet, C. Torres, *J. Antimicrob. Chemother.* **2012**, *67*, 886 – 897.

[31] C. Lozano, C. Aspiroz, A. I. Ezpeleta, E. Gomez-Sanz, M. Zarazaga, C. Torres, *Emerging Infect. Dis.* **2011**, *17*, 138 – 140.

Received: February 17, 2016
Published online on June 3, 2016

